HHS Public Access

Author manuscript

Neuropharmacology. Author manuscript; available in PMC 2019 December 01.

Published in final edited form as:

Neuropharmacology. 2018 December ; 143: 113–121. doi:10.1016/j.neuropharm.2018.09.031.

Neurotensin and Dynorphin Bi-Directionally Modulate CeA Inhibition of oval BNST Neurons in Male Mice

CP Normandeau[1], **ML Torruella Suárez**[2], **P Sarret**[3], **ZA McElligott**[*,4], and **EC Dumont**[*,1]

[1]Department of Biomedical and Molecular Sciences, Queen's University, Kingston, ON, Canada

[2]Program in Neurobiology, School of Medicine, University of North Carolina at Chapel Hill

[3]Department of Pharmacology & Physiology, Faculty of Medicine and Health Sciences, Université de Sherbrooke, Sherbrooke, QC, Canada

[4]Bowles Center for Alcohol Studies and Departments of Psychiatry and Pharmacology, School of Medicine, University of North Carolina at Chapel Hill, USA

Abstract

Neuropeptides are often co-expressed in neurons, and may therefore be working together to coordinate proper neural circuit function. However, neurophysiological effects of neuropeptides are commonly studied individually possibly underestimating their modulatory roles. Here, we triggered the release of endogenous neuropeptides in brain slices from male mice to better understand their modulation of central amygdala (CeA) inhibitory inputs onto oval (ov) BNST neurons. We found that locally-released neurotensin (NT) and dynorphin (Dyn) antagonistically regulated CeA inhibitory inputs onto ovBNST neurons. NT and Dyn respectively increased and decreased CeA-to-ovBNST inhibitory inputs through NT receptor 1 (NTR1) and kappa opioid receptor (KOR). Additionally, NT and Dyn mRNAs were highly co-localized in ovBNST neurons suggesting that they may be released from the same cells. Together, we showed that NT and Dyn are key modulators of CeA inputs to ovBNST, paving the way to determine whether different conditions or states can alter the neuropeptidergic regulation of this particular brain circuit.

Keywords

neuropeptides; neurotensin; dynorphin; GABA; ovBNST; CeA

1. Introduction

Neuropeptides are frequently co-expressed in individual neurons within the nervous system; their cooperative role may enable flexible neuromodulation and proper function of neural

Corresponding author: Dr. Éric C. Dumont (eric.dumont@queensu.ca).
*Both authors contributed equally as senior authors

Financial interest or conflict of interest: the authors have no financial or conflict of interest.

circuits (Griebel and Holsboer, 2012; Kormos and Gaszner, 2013; Valentino and Aston-Jones, 2010). However, neuropeptides are often studied individually, neglecting the functional outcomes resulting from their coordinated actions (Ptak et al., 2009; Sun et al., 2003). In brain slices prepared from male rats, postsynaptic activation of oval bed nucleus of the stria terminalis (ovBNST) neurons triggers the release of various neuropeptides, such as neurotensin (NT), corticotrophin releasing factor (CRF) and dynorphin (Dyn) which in turn robustly modulate excitatory and inhibitory synaptic transmission onto the same neurons (Normandeau et al., 2018). Notably, endogenously-released NT produces an increase in inhibitory transmission in the rat ovBNST, that is further enhanced by chronic stress (Normandeau et al., 2018). What remains unknown is whether this coordinated modulation of synaptic transmission is circuit-specific.

Although still under debate, the ovBNST may be devoted to energy homeostasis, promoting foraging behaviours and food intake (Jennings et al., 2013; Li and Kirouac, 2008; Moga et al., 1995). Located in the dorsolateral region of the BNST, the ovBNST is robustly and reciprocally connected with the central nucleus of the amygdala (CeA), and since these bi-directional connections are exclusively GABAergic, the ovBNST and the CeA most likely inhibit each other (Petrovich and Swanson, 1997). This connection may be integral in the balance between aversive or appetitive behaviours (Davis et al., 2010; Dong et al., 2001; Jennings et al., 2013). Whether neuropeptides are important modulators of this particular brain circuit is largely undetermined. Nonetheless, it is known that the opiate dynorphin (Dyn) released from GABA neurons specifically decreases CeA-to-dorsal BNST inhibitory inputs in male mice (Li et al., 2012). Whether other neuropeptides in the ovBNST regulate CeA inhibition is currently unknown.

Using brain slice electrophysiology in male mice, we triggered endogenous release of neuropeptides and discovered that release of NT and Dyn had opposing effects on CeA-to-ovBNST synaptic inhibition through neurotensin receptors 1 (NTR1) and kappa opioid receptors (KOR), respectively. NT-mediated enhancement of inhibitory transmission in the ovBNST overshadowed the effect of Dyn, paving the way to determine whether changes in condition/state may affect neuropeptidergic regulation of synaptic transmission in this particular neural circuit.

2. Materials and Methods

2.1. Mice

46 mice (>8 weeks old) were group housed on a reverse 12-hour light/dark cycle (lights OFF at 8:00 A.M) with *ad libitum* access to chow and water. C57BL/6J adult male mice (n=29) used for electrophysiology were obtained from Charles River Laboratories (St-Constant, QC, Canada) and *Vgat-Cre* adult male mice (n=17) used for electrophysiology and *in situ* hybridization were bred in house in the McElligott lab (University of North Carolina, Chapel Hill, NC, USA). *Vgat-Cre* mice were obtained from Jackson Labs (originally generated by Bradford Lowell, Harvard University), and the virus lot #43140 was generated at UNC Chapel Hill. All experiments were conducted in accordance to the guidelines from the Canadian Council on Animal Care in Science, approved by Queen's University, and were in accordance with the National Institutes of Health guidelines for animal research with the

approval of the Institutional Animal Care and Use Committee at the University of North Carolina at Chapel Hill.

2.2. Stereotaxic injections

Mice were deeply anesthetized with 3% isoflurane (vol/vol) in oxygen, placed into a stereotactic frame (Kopf Instruments, Tujunga, CA, USA) and maintained at 1.5–2.5% isoflurane during surgery. A hole was drilled in the skull using CeA coordinates ML: ±2,95, AP: −1.15, DV: −4.75 from Bregma. Microinjections of 300 nL of virus (AAV5-EF1a-DIO-ChR2-mCherry or AAV5-EF1a-DIO-ChR2-eYFP) were made bilaterally using a 1 μl Neuros Hamilton syringe (Hamilton, Reno, NV, USA) at a rate of 100 nl/minute. After infusion, the needle was left in place for at least an additional 5 minutes to allow complete diffusion of the virus before being slowly withdrawn. After surgery, all mice were returned to group housing, and recovered for at least 6 weeks prior to the start of experiments.

2.3. Slices preparation and electrophysiology

Mice were anesthetized with isoflurane (5% at 5 L/minute) and their brain removed into ice-cold artificial cerebral spinal fluid (aCSF) containing (in mM): 126 NaCl, 2.5 KCl, 1.2 MgCl2, 6 CaCl2, 1.2 NaH2PO4, 25 NaHCO3, and 12.5 D-glucose equilibrated with 95% O2/5% CO2. Brains were cut in 2°C aCSF into coronal slices (300 μm) with a vibrating blade microtome (VT-1000; Leica Canada, Concord, ON, Canada). The ovBNST slice of interest for this study corresponded to −0.26mm from Bregma. Slices were made of CeA to verify viral injection cites in all *vGAT-cre* animals. Slices were incubated at 34°C for 60 minutes and transferred to a chamber perfused (2-3 mls/minute) with aCSF at 34°C. Remaining slices were kept in aCSF at room temperature until further use. Whole-cell voltage-clamp recordings were made using glass microelectrodes (3–5 MΩ) filled with (in mM): 70 K+-gluconate, 80 KCl, 1 EGTA, 5 HEPES, 2 MgATP, 0.3 GTP, and 1 P-creatine. Electrical stimuli (10–100 μA, 0.1 ms duration) or optical stimuli (490 nm LED intensity 2-100%, 0.1 ms duration) were applied at 0.1 Hz. Inhibitory postsynaptic currents (IPSCs) were evoked by local fiber stimulation with tungsten bipolar electrodes or by a 490 nm LED via the objective while neurons were voltage-clamped at −70 mV. $GABA_A$-IPSCs were pharmacologically isolated with 6,7-dinitroquinoxaline-2,3-dione (DNQX, 50 μM). To induce local endogenous neuropeptide release, postsynaptic neurons were repetitively depolarized in voltage clamp from −70 to 0 mV (100 ms) at a frequency of 2 Hz for 5 minutes (Normandeau et al., 2018). We quantified peak amplitude and defined 3 possible outcomes to postsynaptic depolarization or drug bath application: 1-long-term potentiation (LTP^{GABA}; >20% increase from baseline after 20 minutes), 2-long-term depression (LTD^{GABA}; <20% decrease from baseline after 20 minutes) or 3-no change (NC, within 20% deviation from baseline after 20 minutes) (Normandeau et al., 2018). Recordings were made using a Multiclamp 700B amplifier and a Digidata 1440A (Molecular Devices LLC, San Jose, CA, USA). Data were acquired and analyzed with Axograph X running on Apple computers and Clampex on Windows computers.

2.4. Drugs

Stock solutions of SR142948 (10 mM), Norbinaltorphimine (Nor-BNI, 100 mM), NT (1mM) and JMV431 (1mM) were prepred in distilled water. Stock solutions of DNQX (100

mM), and NTRC844 (1mM) were prepared in DMSO (100%). All drugs were further dissolved in the physiological solutions at the desired concentrations (DNQX 50μM, SR142948 10 μM, Nor-BNI, 100 nM, JMV431 100nM, NTRC844 100nM, SR48692 1μM, NT 1μM) and the final DMSO concentration never exceeded 0.1%.

2.5 Fluorescence *In Situ* Hybridization (FISH)

Immediately after removal, brains were placed on a square of aluminum foil on dry ice to freeze for 5 minutes before wrapping to prevent tissue damage. Brains were then placed in a −80 °C freezer for no more than 1 week before slicing. In all, 12-μm slices containing the CeA and ovBNST were obtained on a Leica CM3050S cryostat (Leica Biosystems, Wetzlar, Germany) and placed directly on coverslips. FISH was performed using the Affymetrix ViewRNA 2-Plex Tissue Assay Kit with custom probes for *Pdyn, Nts, Ntsr1,* and *Ntsr2* designed by Affymetrix (Santa Clara, CA, USA). FISH was also done using the Advanced Cell Diagnostics (ACD) HybEZ(TM) II Hybridization System with custom probes for *Nts* and *Pdyn* designed by ACD (Newark, CA, USA). Slides were coverslipped with SouthernBiotech DAPI Fluoromount-G. (Birmingham, AL, USA). z-Stack (3 × 5 tiled; 8 optical sections comprising 10.57 μm in total) were obtained on a Zeiss 800 confocal microscope. All images were preprocessed with stitching and maximum intensity projection. Quantification of probe colocalization was hand counted using the cell counter plugin in FIJI (ImageJ, NIH, Bethesda, MD, USA). For all studies, cells were classified into three groups: probe 1+, probe 2+ or probe 1 + and 2+. Co-localization ratio was calculated by (probe 1+ and probe 2+/probe 1+ or probe 2+)*100 (McCullough et al., 2018).

2.6 Statistical analyses

Changes in IPSCs peak amplitude were measured from baseline and are shown as percentage change from baseline: $((\text{Peakamplitude}_{post} - \text{Peakamplitude}_{baseline})/\text{Peakamplitude}_{baseline})*100-100$. Data are reported as means ± SEM and each data point represents the average of values in 1-minute bins (6 evoked IPSCs) across recorded neurons. ANOVAs were used to compare multiple means and the appropriate post-hoc statistical tests for multiple comparisons conducted when ANOVAs deemed significance. All statistics from the within-subjects ANOVAs were reported using the Greenhouse-Guesser correction for violations in sphericity, and degrees of freedom for Greenhouse-Giesser values were rounded up to the nearest whole number. A Bonferroni correction was used for multiple comparisons. Fisher's exact tests analyzed contingency tables of the neuronal response distribution. All statistical analyses were done with SPSS Statistics Version 23 (SAS Institute) or Prism 6 (Graph Pad).

3. Results

Multiple neuropeptides are usually co-expressed in individual neurons in the brain, suggesting concerted roles in coordinating proper neural circuit function. However, whether and how multiple neuropeptidergic systems interact neurophysiologically to regulate neural circuits is largely unknown. Here, we triggered release of endogenous neuropeptides in ovBNST brain slices to investigate how neuropeptides can regulate CeA to ovBNST inhibitory circuit in male mice.

3.1. Bi-directional modulation of electrically-evoked GABA-IPSCs by NT and Dyn in the ovBNST of male mice

Electrical stimulation of local fibers evoked $GABA_A$-IPSCs (eIPSCs) in ovBNST neurons and peak amplitudes were measured. Upon stable baseline of eIPSCs (minimum 5 minutes), postsynaptic ovBNST neurons were activated for 5 minutes by repetitive depolarization (0mV, 100msec, 2Hz), which resulted in long-term potentiation (LTP^{GABA}) of eIPSCs in 90% of recorded neurons (time x group, $F_{3,8}$=9.5, p=0.002; Figure 1B). The addition of non-selective NTRs antagonist (SR-142948, 10μM) diminished LTP^{GABA} cell response indicating that NT is an important modulator of inhibitory transmission in mice (Fisher's exact test (aCSF vs. SR); p=0.04; Figure 1C, E). Blocking NT receptors also uncovered LTD^{GABA} that was ablated by co-application of the selective KOR antagonist nor-NBI (100nM) with SR (time × group, $F_{1,9}$=31.6, p=0.0003; Figure 1D, E). As such, locally released NT and Dyn inversely regulate inhibitory transmission in the ovBNST.

3.2. Locally released NT and Dyn target CeA-to-ovBNST GABA synaptic transmission

Next, using *Vgat-Cre* male mice injected with DIO-ChR2-eYFP/mCherry in the CeA, we light-activated (LED 490nm) CeA inputs and evoked optical $Vgat^{CeA \rightarrow ovBNST}$GABA-IPSCs (opIPSCs) in ovBNST neurons. Because our repetitive depolarization protocol requires activity within the slice, we were precluded from making our recordings in sodium and potassium channel blockers to isolate circuitry. Thus, we specifically targeted GABA neurons with the *vGAT-cre* to reduce the chance of polysynaptic activity that may occur if a mix of GABA and glutamate neurons (from area like the BLA) were transduced with a less selective virus. Postsynaptic activation of ovBNST neurons by repetitive depolarization resulted in 54% LTP^{GABA} of opIPSCs and 8% LTD^{GABA} (time × group, $F_{5,20}$=4.1, p=0.01; Figure 2C). Application of the non-selective NTRs antagonist robustly reduced LTP^{GABA} (8%) and revealed further LTD^{GABA} (42%, Fisher's exact test (aCSF vs. SR), p=0.04; Figure 2D,F). Combined application of NTRs and KOR antagonist completely eliminated LTP^{GABA} and LTD^{GABA} and LTD^{GABA} cell responses (Fisher's exact test (SR vs. SR/norNBI), p=0.04; Figure 2E,F). These data suggest that, NT and Dyn are the dominant modulators of CeA inputs onto ovBNST in mice.

3.3. Expression of *Nts* and *Pdyn* mRNA co-localized in the ovBNST

We then determined whether preprodynorphin (*Pdyn*) and NT (*Nts*) mRNA are expressed in the same or different cell populations in the ovBNST. Dual fluorescent *in situ* hybridization (FISH) revealed strong co-localization of *Pdyn* in *Nts* mRNA probe positive neurons in the ovBNST (67.3%±2.1%, Figure 3). Suggesting the majority of cells expressing *Nts* in the ovBNST will also express *Pdyn.*

3.4. NTR1 and NTR2 bi-directionally modulated eIPSCs in the ovBNST

NT binds to two different G-protein receptors on the cell surface: NTR1 and NTR2 (Vincent et al., 1999). Both *Ntsr1* and *Ntsr2* mRNA were present in the ovBNST and CeA (Figure 4A-H). However, neither *Ntsr1* nor *Ntsr2* co-localized extensively with *Nts* mRNA in probe positive neurons suggesting that NT released by the repetitive depolarization paradigm signaled heterosynaptically on a distinct population of NTR-positive neurons in the

ovBNST. Consistent with what we observed with the repetitive depolarization paradigm, pharmacological application of NT (1 μM) for 5 minutes resulted in LTP^{GABA} of eIPSCs in 80% of recorded neurons (time, $F_{1,46}$=8.3, p=0.002; Figure 5A). Bath application of the NTR2 selective antagonist (NTRC844, 100nM) did not significantly alter the percent of cells exhibiting LTP^{GABA} to a subsequent 5 minute bath application of NT, with 57% of cells responding with LTP^{GABA} (Fisher's exact test (NT vs. NT+NTRC844), p=0.6; Figure 5B, E) (Thomas et al., 2016). Bath application of the NTR1 selective antagonist (SR48692, 1μM), however, did not result in any LTP^{GABA} neuron response following the 5 minute NT bath application (Fisher's exact test (NT vs. NT +SR48692), p=0.002; Figure 5C, E), suggesting that NTR1 is required for the NT-mediated LTP^{GABA} response following repetitive depolarization. The blockade of NTR1 also uncovered LTD^{GABA} in 80% of neurons that could be NTR2 mediated. Accordingly, bath application of the NTR2 selective agonist (JMV431, 100nM) for 5 minutes resulted in a LTD^{GABA} in 38% of neurons (time × group, $F_{6,35}$=3.4, p=0.04; Figure 5D) (Thomas et al., 2014). Overall, our data demonstrates that NTRs have opposing modulatory roles on inhibitory transmission in the ovBNST, although the NTR1 component was predominant in response to endogenous NT release.

4. Discussion

Postsynaptic depolarization of ovBNST neurons in male mice brain slices resulted in the putative release of the neuropeptides NT and Dyn, respectively increasing and decreasing inhibitory inputs originating in the CeA. FISH revealed that *Nts* and *Pdyn* mRNA significantly overlapped in single ovBNST cells demonstrating the co-localization of NT and Dyn in the ovBNST. Locally released NT and Dyn modulated CeA inhibition of ovBNST neurons through NTR1 and KOR respectively, although the effect of NT overshadowed that of Dyn. Together, our data shed new light unto the coordinated action of co-localized neuropeptides in fine-tuning neural circuit function.

Postsynaptic activation resulted in endogenous release of neuropeptides

Postsynaptic activation of voltage-clamped ovBNST neurons resulted in a robust and long-lasting modulation of inhibitory postsynaptic $GABA_A$ currents in a vast majority (up to 90%) of recorded neurons. We hypothesized that this effect could be neuropeptide mediated since they are generally released after high or prolonged postsynaptic depolarization, and have long-lasting effects (Karhunen et al., 2001; Whim and Lloyd, 1989). Pharmacological blockade of NTR and KOR receptors confirmed that NT and Dyn were fully responsible for the lasting bi-directional regulation of ovBNST inhibitory inputs from the CeA. In male rats, the same postsynaptic activation protocol (2Hz, 5 minutes) also triggered local endogenous neuropeptides release and similar modulation of inhibitory synaptic transmission in the ovBNST, suggesting a conserved mechanism across both species (Normandeau et al., 2018). Although our data do not preclude the presence of other neuromodulators (for example endocannabinoids, growth factors, or other neuropeptides), the modulation of inhibitory synaptic transmission was largely eliminated by the co-application of NTR and KOR antagonists. Thus, we believe these observed effects were predominantly NT- and Dyn-dependent.

Postsynaptic activation resulted in homogenous NT response in electrically evoked IPSCs

Postsynaptic activation resulted in a strikingly homogenous NT-mediated (over 90% of the cells) enhancement of inhibitory transmission in the ovBNST. This is consistent with the prevalence of NT-positive neurons in the ovBNST, although may seem to contrast with the various neurophysiological signatures reported in the rat dorsal BNST neurons (Allen Mouse Brain Atlas, Hammack et al., 2007; Ju et al., 1989). However, a majority of dorsal BNST neurons express the neuropeptide CRF that is co-expressed with NT regardless of neurophysiological signature (Dabrowska et al., 2013; Hammack et al., 2007; Ju and Han, 1989). Thus, these neuropeptides may be acting on a variety of cell types with the same neurophysiological outcome, and may enable the ovBNST to function in a coordinated network fashion (Larriva-Sahd, 2006).

Differences in modulation between electrically evoked and optically evoked inputs

Narrowing our investigation to CeA-mediated optically-driven (op)IPSCs revealed that postsynaptic depolarization correspondingly resulted in robust modulation of inhibitory afferents onto ovBNST neurons. Although at a lower proportion than non-specific (eIPSC) input stimulation, a majority of neurons (54%) displayed LTP^{GABA} of similar magnitude and duration. In contrast, LTD^{GABA} was more readily observable with opIPSCs (8% of neurons) without NTRs blockade. Similar to eIPSC, NTR blockade fully revealed KOR-mediated LTD^{GABA}. Co-application of NTR and KOR antagonists completely abolished the modulation of opIPSCs whereas a residual LTP^{GABA} remained with electrical stimulation (45%). In male rats, a similar residual eIPSC LTP^{GABA} was mediated by CRF, and we suspect this neuropeptide may also be responsible for the residual LTP^{GABA} observed in mice (Normandeau et al., 2018). Notably, since ovBNST neurons patched were not labeled for neuropeptide content, there is some variability likely attributed to cell viability (i.e. viability following slicing, experimenter preference for certain cell appearance, etc.). Nonetheless, our findings strongly suggest that NT and Dyn are fully responsible for bi-directional modulation of CeA inhibitory inputs to ovBNST neurons in male mice (Li et al., 2012).

Dyn and NT co-localize in the ovBNST

Cells containing *Nts* mRNA were highly co-localized with *Pdyn* mRNA in ovBNST, suggesting that both neuropeptides could be released from the same cells to have their modulatory effects. Importantly, however, mRNA abundance does not necessarily translate 1:1 to protein expression, nor does it inform how neuropeptides are packaged or released under depolarizing conditions. Therefore, further investigation is necessary to understand whether NT and Dyn are packaged in the same or different vesicles, and if they are released together or separately.

Furthermore, neither neuropeptides' mRNA (*Nts* or *Pdyn*) co-localize significantly with their respective receptors mRNA. There is a high concentration of *Oprk1* mRNA expression in the CeA and not the ovBNST (DePaoli et al., 1994; Poulin et al., 2009). While *Ntsr1* and *Ntsr2* mRNA were expressed in both ovBNST and CeA neurons. Therefore, the neuropeptides may act on pre-synaptic axon terminals from the CeA (illustrated in Figure 6), however, we cannot exclude the possibility that NT may be working through interneurons

since we identified *Ntsr* mRNA in the ovBNST. Additionally, *Ntsr2* may be expressed on non-neuronal cell types for example glial cells (Woodworth et al., 2017; Yamauchi et al., 2007). However, the exact cellular localization of NTS2 is still contentious, as they have also been identified in ependymal cells (Lepee-Lorgeoux et al., 1999; Walker et al., 1998).

Upon release, NT and Dyn may independently modulate inhibition in the ovBNST by acting at their respective receptors. Alternatively, they may also interact directly since KOR and NTR1 can form heterodimers that alters KOR-mediated signaling (Liu et al., 2016). In fact, KOR and NTR1 are both expressed in the CeA and could co-localize pre-synaptically in ovBNST inputs (Boudin et al., 1996; Mansour et al., 1987). While the exact functional link between NT and Dyn remains elusive, it is clear that the two neuropeptides have strong antagonistic potential to regulate inhibition in the ovBNST.

NTR1 and NTR2 opposing modulation of inhibitory transmission in the ovBNST

Seeing that NT could be acting on both NTR1 and NTR2, we investigated which receptor could be responsible for its modulatory effect. First, bath-application of exogenous NT resulted in LTP^{GABA} in 80% of recorded ovBNST neurons, similar to our previous observation in rats (Krawczyk et al., 2013). Next, NTR1 (SR48692), but not NTR2 (NTRC844), blockade, significantly interfered with NT-induced LTP^{GABA} suggesting this response is NTR1 mediated. Interestingly, blockade of NTR1 also uncovered LTD^{GABA} and application of NTR2 selective agonist JMV431 resulted in LTD^{GABA} in 38% of recorded neurons. Thus, NTR2 activation reduces inhibitory transmission in the ovBNST, and acts opposite to NTR1. Importantly, this is the first observation of NTR2 modulated effects on GABA transmission.

Our postsynaptic activation only detected NT-mediated LTP^{GABA} however, since the LTD^{GABA} observed was in the presence of NTR non-selective antagonist. NT has a higher affinity to NTR1 than NTR2, suggesting that postsynaptic depolarization may release low to moderate amounts of endogenous NT that may only activate NTR1s (Tschumi and Beckstead, 2018). Additionally, NTR2 are preferentially expressed intra-cellularly whereas NTR1s are expressed at the cell membrane, potentially increasing NT's ability to bind and activate NTR1s (Perron et al., 2007). Overall, NTR1 predominantly mediated the modulation of inhibitory transmission after postsynaptic activation in our experimental preparation.

NT overshadowed Dyn modulation

With either stimulation of local fibers or CeA inputs, the blockade of NTR1 uncovered Dyn-induced LTD^{GABA}. Consequently, NT seems to be the primary modulator of CeA inhibitory inputs onto ovBNST neurons. Our stimulation paradigm (2Hz, 5minutes) could particularly favor NT over Dyn release, as previous research suggests that different firing patterns can release different neuropeptides (Poulain et al., 1977). Alternatively, the relative availability of neuropeptides and receptor expression or function may be state-dependent. In our experiments, the mice were sated, not manipulated for stress, and brain slices were prepared approximately 2 hours within the active (dark) phase of the mouse circadian cycle. Because the ovBNST seems important for energy homeostasis and is a one of the brain's circadian

clock, it will be critical to determine whether Dyn-mediated LTD^{GABA} may not become the primary response in different conditions (Amir et al., 2004; Dong et al., 2001).

Role of Dyn and NT in CeA and ovBNST neural circuit

Anatomical studies suggest that the CeA and ovBNST robustly inhibit one another such that their physiological roles are possibly antagonistic (Dong et al., 2001; Petrovich and Swanson, 1997). The CeA is instrumental in promoting aversive learning and fear response whereas the dorsolateral BNST might be more related to appetitive behaviours (Davis et al., 2010; Jennings et al., 2013). Energy homeostasis may be an important factor in the neuromodulatory effects of NT vs. Dyn on the CeA-to-ovBNST circuit. For instance, they have opposing effects on foraging behaviours: NT and Dyn respectively decrease and increase food intake in both rats and mice (Cooke et al., 2009; Lambert et al., 1993; Levine et al., 1983; Luttinger et al., 1982; Sainsbury et al., 2007). Intriguingly, NT reduces Dyn-induced feeding in rats (Levine et al., 1983). Furthermore, NT and Dyn expression and release are metabolic state-dependent. In rats, NT release into the hepatic-portal circulation occurs immediately after cessation of eating (George et al., 1987). In contrast, Dyn expression increases significantly in the rat hypothalamus after a 72-hour food deprivation (Przewlocki et al., 1983). Therefore, NT may promote CeA inhibition of the ovBNST to decrease foraging behaviour.

5. Conclusion

In sum, our data strongly suggest that NT and Dyn both fine-tune CeA inhibitory inputs onto ovBNST neurons. We have described one circuit, as well as two co-expressed behaviorally-relevant neuropeptides that may serve as a source of bi-directional modulation *in vivo.* Our study paves the way to investigate whether similar phenomenon occurs in other neuropeptidergic systems, and if it can be generalized outside of the extended amygdala.

Acknowledgements.

This work was supported by the Canadian Institute of Health Research Vanier Graduate Scholarship (338319), Canadian Institute of Health Research (MOP-25953, FDN-148413), Canada Research Chair in Neurophysiopharmacology of Chronic Pain, National Institutes of Alcohol Abuse and Alcoholism (K01AA02355), Alcohol Beverage Medical Research Foundation, NCTRacS (550KR71419), National Institute of Neurological Disorders and Stroke (T32NS007431).

References

Amir S, Lamont EW, Robinson B, Stewart J, 2004 A circadian rhythm in the expression of PERIOD2 protein reveals a novel SCN-controlled oscillator in the oval nucleus of the bed nucleus of the stria terminalis. J Neurosci 24, 781–790. [PubMed: 14749422]

Boudin H, Pelaprat D, Rostene W, Beaudet A, 1996 Cellular distribution of neurotensin receptors in rat brain: immunohistochemical study using an antipeptide antibody against the cloned high affinity receptor. J Comp Neurol 373, 76–89. [PubMed: 8876464]

Cooke JH, Patterson M, Patel SR, Smith KL, Ghatei MA, Bloom SR, Murphy KG, 2009 Peripheral and central administration of xenin and neurotensin suppress food intake in rodents. Obesity (Silver Spring) 17, 1135–1143. [PubMed: 19214175]

Dabrowska J, Hazra R, Guo JD, Li C, Dewitt S, Xu J, Lombroso PJ, Rainnie DG, 2013 Striatal-enriched protein tyrosine phosphatase-STEPs toward understanding chronic stress-induced

activation of corticotrophin releasing factor neurons in the rat bed nucleus of the stria terminalis. Biol Psychiatry 74, 817–826. [PubMed: 24012328]

Davis M, Walker DL, Miles L, Grillon C, 2010 Phasic vs sustained fear in rats and humans: role of the extended amygdala in fear vs anxiety. Neuropsychopharmacology 35, 105–135. [PubMed: 19693004]

DePaoli AM, Hurley KM, Yasada K, Reisine T, Bell G, 1994 Distribution of kappa opioid receptor mRNA in adult mouse brain: an in situ hybridization histochemistry study. Mol Cell Neurosci 5, 327–335. [PubMed: 7804602]

Dong HW, Petrovich GD, Watts AG, Swanson LW, 2001 Basic organization of projections from the oval and fusiform nuclei of the bed nuclei of the stria terminalis in adult rat brain. J Comp Neurol 436, 430–455. [PubMed: 11447588]

George JK, Albers HE, Carraway RE, Ferris CF, 1987 Neurotensin levels in the hepatic-portal circulation are inversely related to the circadian feeding cycle in rats. Endocrinology 121, 7–13. [PubMed: 3595525]

Griebel G, Holsboer F, 2012 Neuropeptide receptor ligands as drugs for psychiatric diseases: the end of the beginning? Nature Reviews Drug Discovery 11, 462–478. [PubMed: 22596253]

Hammack SE, Mania I, Rainnie DG, 2007 Differential expression of intrinsic membrane currents in defined cell types of the anterolateral bed nucleus of the stria terminalis. J Neurophysiol 98, 638–656. [PubMed: 17537902]

Jennings JH, Rizzi G, Stamatakis AM, Ung RL, Stuber GD, 2013 The inhibitory circuit architecture of the lateral hypothalamus orchestrates feeding. Science 341, 1517–1521. [PubMed: 24072922]

Ju G, Han ZS, 1989 Coexistence of Corticotropin Releasing-Factor and Neurotensin within Oval Nucleus Neurons in the Bed Nuclei of the Stria Terminalis in the Rat. Neurosci Lett 99, 246–250. [PubMed: 2657507]

Ju G, Swanson LW, Simerly RB, 1989 Studies on the cellular architecture of the bed nuclei of the stria terminalis in the rat: II. Chemoarchitecture. J Comp Neurol 280, 603–621. [PubMed: 2468695]

Karhunen T, Vilim FS, Alexeeva V, Weiss KR, Church PJ, 2001 Targeting of peptidergic vesicles in cotransmitting terminals. J Neurosci 21, RC127. [PubMed: 11157098]

Kormos V, Gaszner B, 2013 Role of neuropeptides in anxiety, stress, and depression: from animals to humans. Neuropeptides 47, 401–419. [PubMed: 24210138]

Krawczyk M, Mason X, DeBacker J, Sharma R, Normandeau CP, Hawken ER, Di Prospero C, Chiang C, Martinez A, Jones AA, Doudnikoff E, Caille S, Bezard E, Georges F, Dumont EC, 2013 D1 dopamine receptor-mediated LTP at GABA synapses encodes motivation to self-administer cocaine in rats. J Neurosci 33, 11960–11971. [PubMed: 23864683]

Lambert PD, Wilding JP, al-Dokhayel AA, Bohuon C, Comoy E, Gilbey SG, Bloom SR, 1993 A role for neuropeptide-Y, dynorphin, and noradrenaline in the central control of food intake after food deprivation. Endocrinology 133, 29–32. [PubMed: 8100519]

Larriva-Sahd J, 2006 Histological and cytological study of the bed nuclei of the stria terminalis in adult rat. II. Oval nucleus: extrinsic inputs, cell types, neuropil, and neuronal modules. J Comp Neurol 497, 772–807. [PubMed: 16786552]

Lepee-Lorgeoux I, Betancur C, Rostene W, Pelaprat D, 1999 Differential ontogenetic patterns of levocabastine-sensitive neurotensin NT2 receptors and of NT1 receptors in the rat brain revealed by in situ hybridization. Brain Res Dev Brain Res 113, 115–131. [PubMed: 10064881]

Levine AS, Kneip J, Grace M, Morley JE, 1983 Effect of centrally administered neurotensin on multiple feeding paradigms. Pharmacol Biochem Behav 18, 19–23.

Li C, Pleil KE, Stamatakis AM, Busan S, Vong L, Lowell BB, Stuber GD, Kash TL, 2012 Presynaptic inhibition of gamma-aminobutyric acid release in the bed nucleus of the stria terminalis by kappa opioid receptor signaling. Biol Psychiatry 71, 725–732. [PubMed: 22225848]

Li S, Kirouac GJ, 2008 Projections from the paraventricular nucleus of the thalamus to the forebrain, with special emphasis on the extended amygdala. J Comp Neurol 506, 263–287. [PubMed: 18022956]

Liu H, Tian Y, Ji B, Lu H, Xin Q, Jiang Y, Ding L, Zhang J, Chen J, Bai B, 2016 Heterodimerization of the kappa opioid receptor and neurotensin receptor 1 contributes to a novel beta-arrestin-2-biased pathway. Biochim Biophys Acta 1863, 2719–2738. [PubMed: 27523794]

Luttinger D, King RA, Sheppard D, Strupp J, Nemeroff CB, Prange AJ, Jr., 1982 The effect of neurotensin on food consumption in the rat. Eur J Pharmacol 81, 499–503. [PubMed: 6811292]

Mansour A, Khachaturian H, Lewis ME, Akil H, Watson SJ, 1987 Autoradiographic differentiation of mu, delta, and kappa opioid receptors in the rat forebrain and midbrain. J Neurosci 7, 2445–2464. [PubMed: 3039080]

McCullough KM, Morrison FG, Hartmann J, Carlezon WA, Jr., Ressler KJ, 2018 Quantified Coexpression Analysis of Central Amygdala Subpopulations. eNeuro 5.

Moga MM, Weis RP, Moore RY, 1995 Efferent projections of the paraventricular thalamic nucleus in the rat. J Comp Neurol 359, 221–238. [PubMed: 7499526]

Normandeau CP, Ventura-Silva AP, Hawken ER, Angelis S, Sjaarda C, Liu X, Pego JM, Dumont EC, 2018 A Key Role for Neurotensin in Chronic-Stress-Induced Anxiety-Like Behavior in Rats. Neuropsychopharmacology 43, 285–293. [PubMed: 28649992]

Perron A, Sharif N, Sarret P, Stroh T, Beaudet A, 2007 NTS2 modulates the intracellular distribution and trafficking of NTS1 via heterodimerization. Biochem Biophys Res Commun 353, 582–590. [PubMed: 17188644]

Petrovich GD, Swanson LW, 1997 Projections from the lateral part of the central amygdalar nucleus to the postulated fear conditioning circuit. Brain Res 763, 247–254. [PubMed: 9296566]

Poulain DA, Wakerley JB, Dyball RE, 1977 Electrophysiological differentiation of oxytocin- and vasopressin-secreting neurones. Proc R Soc Lond B Biol Sci 196, 367–384. [PubMed: 17859]

Poulin JF, Arbour D, Laforest S, Drolet G, 2009 Neuroanatomical characterization of endogenous opioids in the bed nucleus of the stria terminalis. Prog Neuropsychopharmacol Biol Psychiatry 33, 1356–1365. [PubMed: 19583989]

Przewlocki R, Lason W, Konecka AM, Gramsch C, Herz A, Reid LD, 1983 The opioid peptide dynorphin, circadian rhythms, and starvation. Science 219, 71–73. [PubMed: 6129699]

Ptak K, Yamanishi T, Aungst J, Milescu LS, Zhang R, Richerson GB, Smith JC, 2009 Raphe neurons stimulate respiratory circuit activity by multiple mechanisms via endogenously released serotonin and substance P. J Neurosci 29, 3720–3737. [PubMed: 19321769]

Sainsbury A, Lin S, McNamara K, Slack K, Enriquez R, Lee NJ, Boey D, Smythe GA, Schwarzer C, Baldock P, Karl T, Lin EJ, Couzens M, Herzog H, 2007 Dynorphin knockout reduces fat mass and increases weight loss during fasting in mice. Mol Endocrinol 21, 1722–1735. [PubMed: 17456788]

Sun QQ, Baraban SC, Prince DA, Huguenard JR, 2003 Target-specific neuropeptide Y-ergic synaptic inhibition and its network consequences within the mammalian thalamus. J Neurosci 23, 9639–9649. [PubMed: 14573544]

Thomas JB, Giddings AM, Wiethe RW, Olepu S, Warner KR, Sarret P, Gendron L, Longpre JM, Zhang Y, Runyon SP, Gilmour BP, 2014 Identification of 1-({[1-(4-fluorophenyl)-5-(2-methoxyphenyl)-1 H-pyrazol-3-yl]carbonyl}amino)cycloh exane carboxylic acid as a selective nonpeptide neurotensin receptor type 2 compound. J Med Chem 57, 5318–5332. [PubMed: 24856674]

Thomas JB, Vivancos M, Giddings AM, Wiethe RW, Warner KR, Murza A, Besserer-Offroy E, Longpre JM, Runyon SP, Decker AM, Gilmour BP, Sarret P, 2016 Identification of 2-({[1-(4-Fluorophenyl)-5-(2-methoxyphenyl)-1H-pyrazol-3-yl]carbonyl}amino)tricyc lo[3.3.1.13,7]decane-2-carboxylic Acid (NTRC-844) as a Selective Antagonist for the Rat Neurotensin Receptor Type 2. ACS Chem Neurosci 7, 1225–1231. [PubMed: 27359371]

Tschumi CW, Beckstead MJ, 2018 Diverse actions of the modulatory peptide neurotensin on central synaptic transmission. Eur J Neurosci.

Valentino R, Aston-Jones G, 2010 Special issue on neuropeptides in stress and addiction: Overview. Brain Res 1314, 1–2. [PubMed: 20141765]

Vincent JP, Mazella J, Kitabgi P, 1999 Neurotensin and neurotensin receptors. Trends Pharmacol Sci 20, 302–309. [PubMed: 10390649]

Walker N, Lepee-Lorgeoux I, Fournier J, Betancur C, Rostene W, Ferrara P, Caput D, 1998 Tissue distribution and cellular localization of the levocabastine-sensitive neurotensin receptor mRNA in adult rat brain. Brain Res Mol Brain Res 57, 193–200. [PubMed: 9675417]

Whim MD, Lloyd PE, 1989 Frequency-dependent release of peptide cotransmitters from identified cholinergic motor neurons in Aplysia. Proc Natl Acad Sci U S A 86, 9034–9038. [PubMed: 2554338]

Woodworth HL, Batchelor HM, Beekly BG, Bugescu R, Brown JA, Kurt G, Fuller PM, Leinninger GM, 2017 Neurotensin Receptor-1 Identifies a Subset of Ventral Tegmental Dopamine Neurons that Coordinates Energy Balance. Cell Rep 20, 1881–1892. [PubMed: 28834751]

Yamauchi R, Wada E, Kamichi S, Yamada D, Maeno H, Delawary M, Nakazawa T, Yamamoto T, Wada K, 2007 Neurotensin type 2 receptor is involved in fear memory in mice. J Neurochem 102, 1669–1676. [PubMed: 17697051]

Highlights:

- Endogenously released NT and Dyn bi-directionally modulate inhibitory CeA inputs to ovBNST through NTR1 and KOR respectively
- NT and Dyn are co-localized in the ovBNST suggesting they are likely released from the same cells to have their modulatory effects
- NTR1 and NTR2 activation have opposing roles in modulating inhibitory transmission in the ovBNST
- First to discover a modulatory role of NTR2 on $GABA_A$ transmission
- Endogenous neuropeptides are multifaceted modulators that should be studied as such

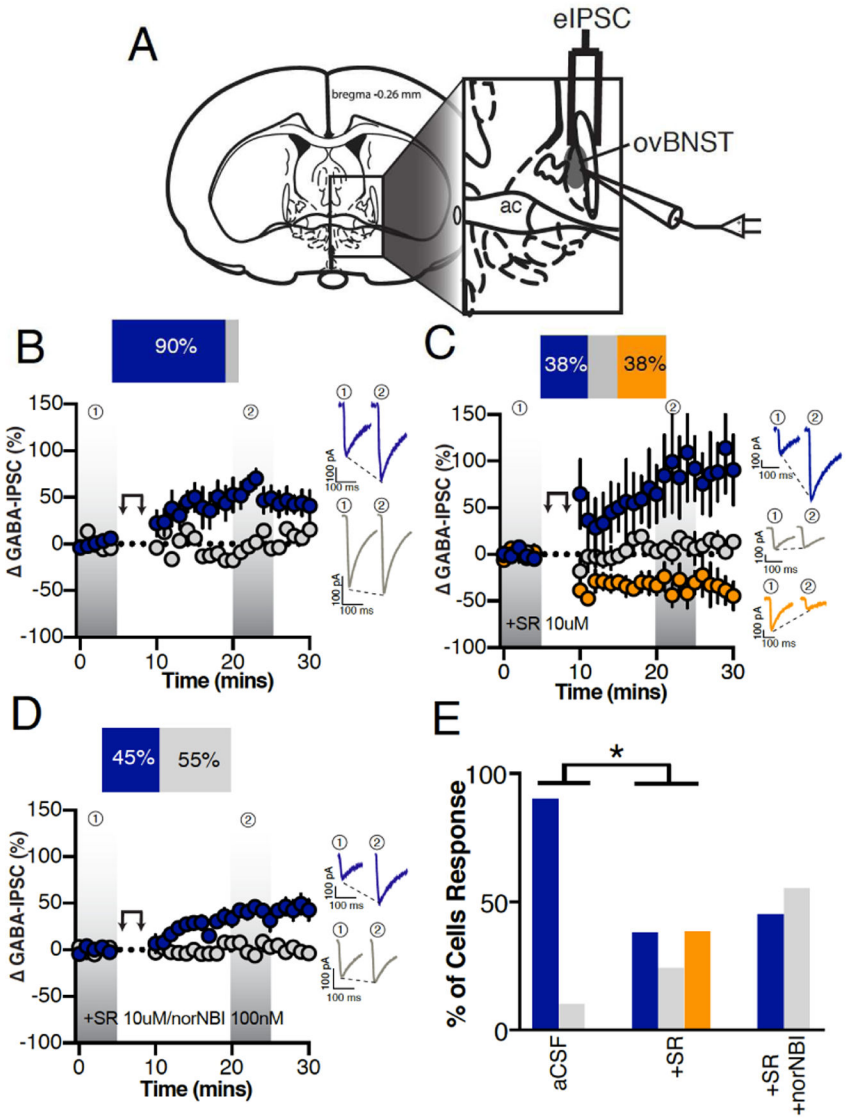

Figure 1. Endogenous neuropeptides modulation of electrically-evoked ovBNST $GABA_A$-IPSCs.

A, Schematic illustrating stimulating and recording electrodes placement in mice brain slices containing the ovBNST. Recordings were restricted to the displayed shaded oval area. B-D, Effects of postsynaptic depolarization (double arrow symbol) on binned (1 minute, 6 events) electrically-evoked $GABA_A$-IPSCs in (B) aCSF (n=10 cells/6 mice), (C) the presence of the non-selective NTR antagonist SR142948 (10μM, n=8 cells/5 mice) or (D) SR142948 + the KOR antagonist norNBI (100nM, n=11 cells/4 mice). Insets in B-D are representative electrically-evoked $GABA_A$-IPSCs before and after postsynaptic depolarization (double arrows). E, Bar graphs summarizing the proportion of responding neurons to postsynaptic depolarization across different pharmacological treatments. Blue LTP, grey no change and orange LTD. Asterisks, $p<0.05$.

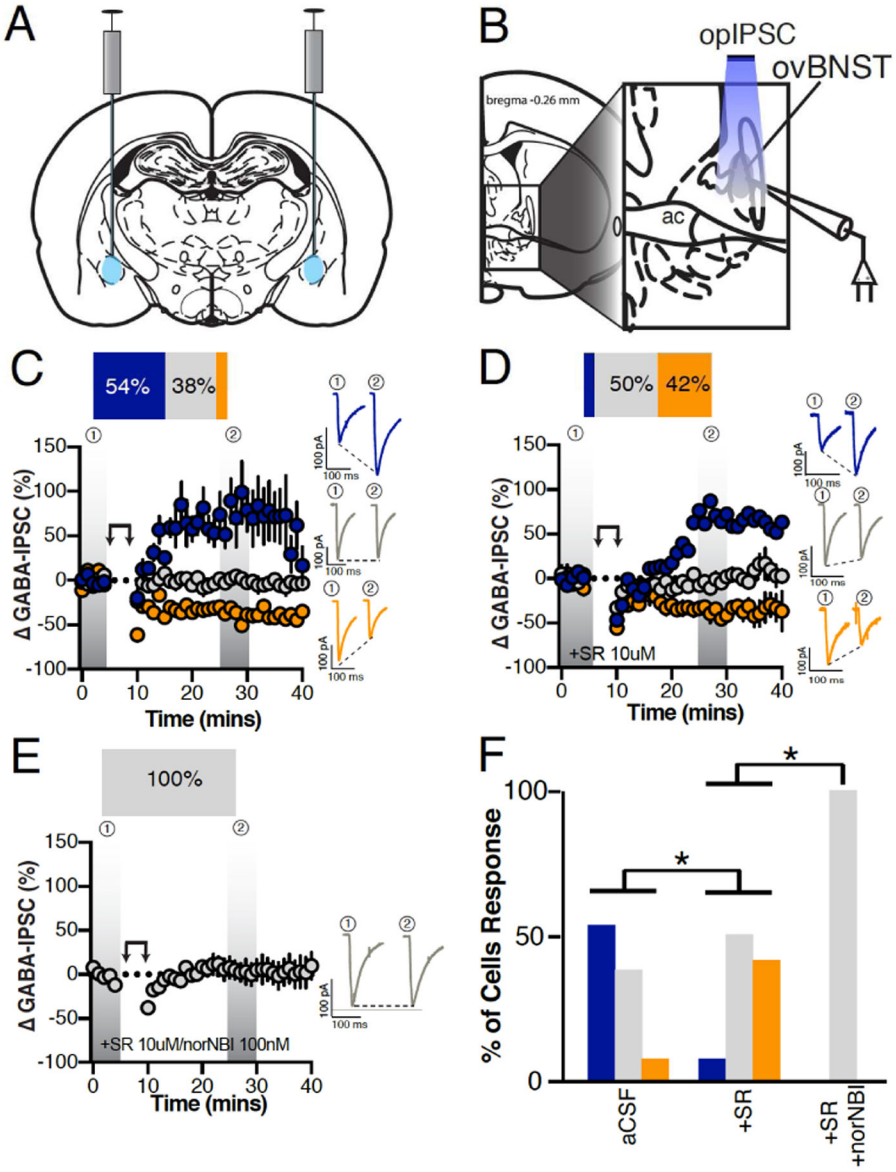

Figure 2. Effect of postsynaptic depolarization on optically-evoked *Vgat*$^{CeA\rightarrow ovBNST}$GABA$_A$-IPSCs.

A, Illustration demonstrating ChR2 bi-lateral injections into the CeA of *Vgat-Cre* mice. B, Illustration demonstrating optically stimulated recordings of ovBNST neurons. C-E, Postsynaptic depolarization in male *Vgat-Cre* mice injected with ChR2 in the CeA and recorded from ovBNST brain slices in (C) aCSF (n=13 cells/6 mice), (D) in the presence of the non-selective NTR antagonist SR142948 (10μM, n=12 cells/5 mice), (E) SR142948 + the KOR antagonist norNBI (100nM, n=8 cells/2 mice). Insets in C-E are representative optically-evoked GABA$_A$-IPSCs before and after postsynaptic depolarization (double arrows). F, Bar graphs summarizing the proportion of responding neurons to postsynaptic depolarization across different pharmacological treatments. Blue LTP, grey no change and orange LTD. Asterisks, $p<0.05$.

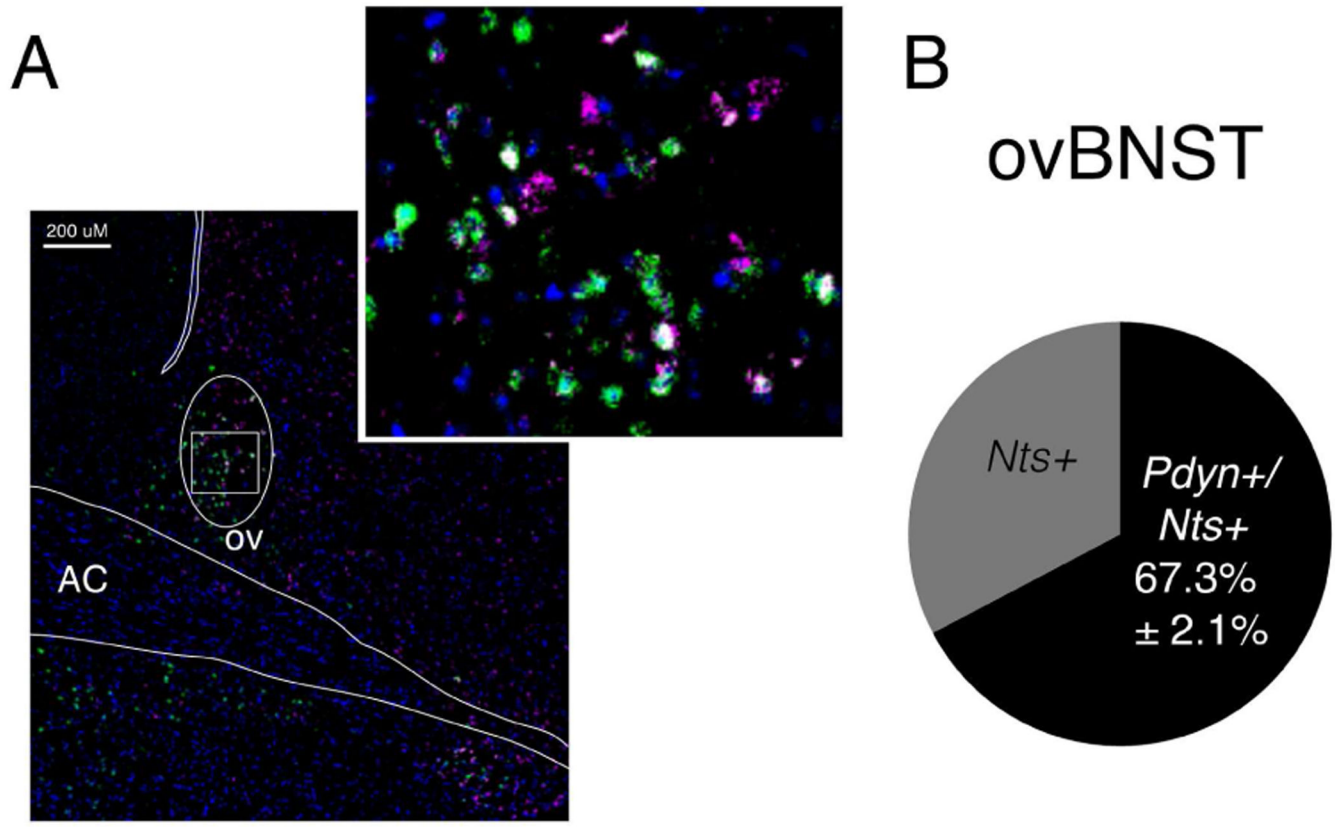

Figure 3. Expression and co-localization of *Pdyn* and *Nts* mRNA in the ovBNST.

A, Representative image of dual fluorescent *in situ* hybridization for *Nts/Pdyn* (*Nts* (green), *Pdyn* (purple), and DAPI (blue)). B, Ratio of the total number of *Nts* mRNA-expressing cells that are positive for *Pdyn* (co-localizing) (average ±SEM % n=4 mice, 4 slices/mouse).

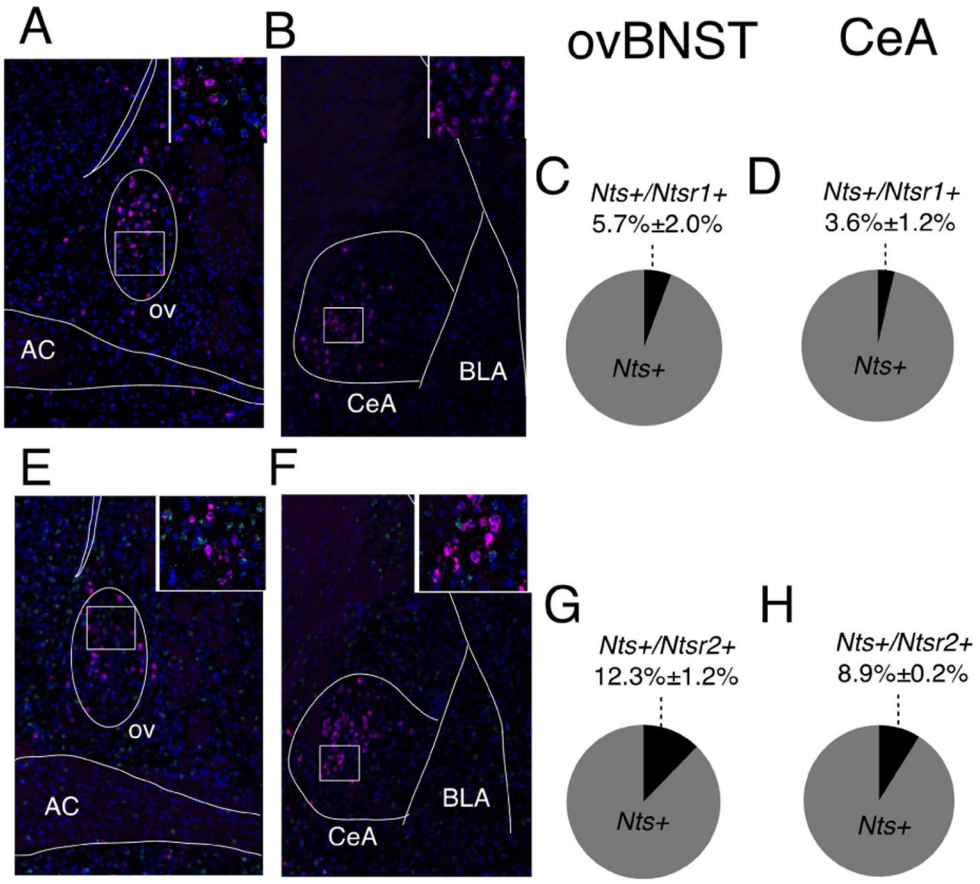

Figure 4. Expression and co-localization of NT and NTRs mRNA in the ovBNST and CeA.
Representative image of dual fluorescent *in situ* hybridization (FISH) for *Nts/Ntsr1* (*Nts* (purple), *Ntsr1* (green), DAPI (blue) in the ovBNST (A) and CeA (B). Ratio of the total number of *Nts* mRNA-expressing cells that are positive for *Ntsr1* (co-localizing) (average ±SEM % n=2 mice, 2 slices/mouse) in the ovBNST (C) and CeA (D). Representative image of dual FISH for *Nts/Ntsr2* (*Nts* (purple), *Ntsr2* (green), DAPI (blue)) in the ovBNST (E) and CeA (F). Ratio of the total number of *Nts* mRNA-expressing cells that are positive for *Ntsr2* (co-localizing) (average ±SEM % n=2 mice, 2 slices/mouse) in the ovBNST (G) and CeA (H).

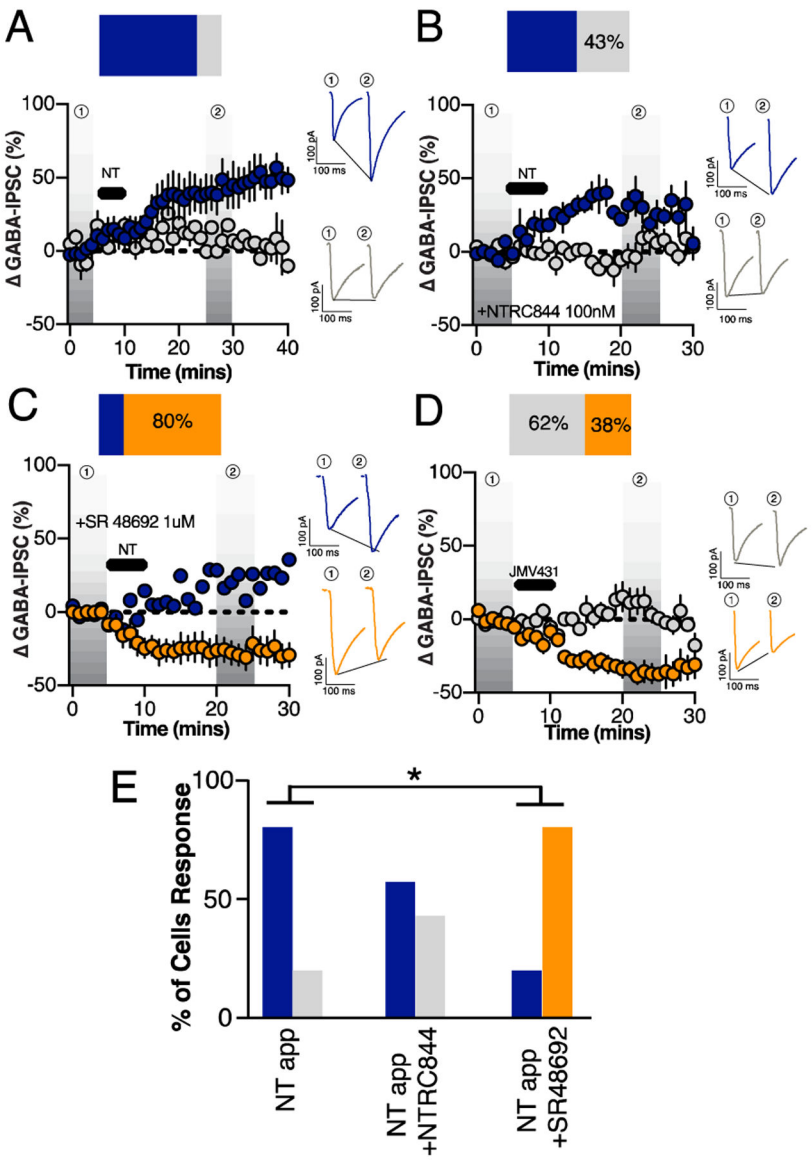

Figure 5. Contribution of neurotensin receptors 1 and 2 on exogenous NT-induced modulation of electrically-evoked ovBNST $GABA_A$-IPSCs.

A, Effect of a 5-minute bath application of NT (1uM) (black horizontal bar) on the peak amplitude of eIPSCs (n=8 cells/4 mice). Effect of NT (1μM, black horizontal bar) on eIPSCs in the presence of (B) the NTR2-selective antagonist NTRC844 (100 nM, n=7 cells/3 mice) or the (C) NTR1-selective antagonist SR48692 (1 μM, n=5 cells/3 mice) D, Effect of a 5-minute bath application of NTR2 agonist JMV431 (100nM, n=8 cells/4 mice) (black horizontal bar) on the peak amplitude of eIPSCs in the ovBNST. Insets in B-D are representative electrically-evoked $GABA_A$-IPSCs before and after bath application of NT or JMV431 for 5 minutes. Bar graphs summarizing the proportion of responding neurons to different pharmacological treatments (E). Blue LTP, grey no change and orange LTD. Asterisks, $p<0.05$.

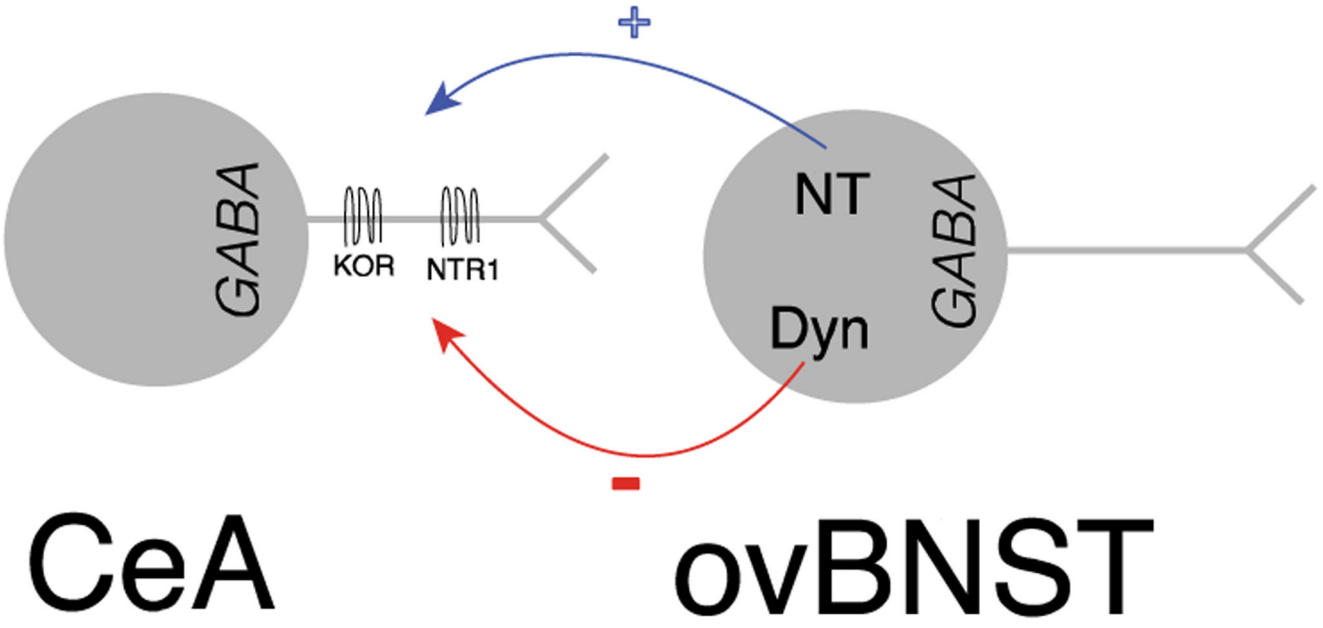

Figure 6.
Illustration of NT and Dyn bi-directional modulation of CeA inputs onto ovBNST neurons.